Research Article

Journal of Chemistry Letters
journal homepage: www.jchemlett.com
ISSN (online) 2717-1892 (print) 2821-0123

Insight into synergistic corrosion inhibition of thiourea and $ZnCl_2$ on mild steel: Experimental and theoretical Approaches

Terngu Timothy Uzah[1, *], Idongesi Justina Mbonu[1]

[1]*Department of Chemistry, College of Science, Federal University of Petroleum Resources, Effurum, Nigeria*

ARTICLE INFO

Article history:
Received 29 August 2023
Received in revised form 4 January 2024
Accepted 4 January 2024
Available online 4 January 2024

Keywords:
DFT
Freundlich
Inhibitor
Thermodynamic
Sulphuric acid

ABSTRACT

Inhibition is the commonest device used to lessen metals and alloys corrosion, especially in acidic media. The synergistic effect of $ZnCl_2$ on the corrosion inhibition efficiency of thiourea on mild steel, in 0.5 M sulfuric acid solution, has been investigated using gravimetric measurements, electrochemical impedance spectroscopy (EIS), scanning electron microscopy (SEM), and Fourier transfer infrared spectroscopy (FTIR) studies as well as density functional theory (DFT) calculations and Monte Carlo simulation. The results show that mild steel inhibition efficiency increase with increasing inhibitor concentrations, and a synergistic enhancement in inhibition efficiencies was observed when $ZnCl_2$ was added. On the surfaces of the corroding metal, inhibitor and inhibitor + $ZnCl_2$ adsorptions follow the Langmuir and Freundlich isotherms, respectively. SEM and FTIR examinations revealed that the metal surface had been coated with an inhibitor, preventing corrosion. The experimental results were agreeably interrelated with theoretical investigations.

1. Introduction

The most popular strategy for reducing the significant economic loss brought on by corrosion is the use of organic inhibitors [1-5]. Additionally, studies are being conducted to determine whether corrosion inhibitors may be used in the environment safely at very low concentrations. In order to achieve a high level of protection efficiency in the presence of a specific inhibitor at low concentrations, secondary molecules and/or ions that enhance the adsorption of an inhibitor via cooperative adsorption or complexation at the surface of the corroded metal are typically required [6-10]. In the current work, the adsorption of thiourea and its potential enhancement in the presence of zinc ions on the surface of mild steel are examined. Amide compounds have historically been acknowledged as powerful inhibitors of corrosion [11-14].

Hence, boosting the thiourea inhibitor solution's adsorption with zinc ions may result in high inhibition efficiency.

2. Results and Discussion

2.1.Quantum Chemical Computations

It is especially helpful to study the structure and property of the inhibitors using the quantum chemistry approach. In accordance with the optimised thiourea structure at B3LYP/6-311G+(d,p), a number of thermodynamic properties can be calculated using Gaussian output files (Figure 1). The portion of the molecule that donates electrons is located in the HOMO [15]. By contrast, the compound's LUMO shows that it can take electrons. Table 1 shows the quantum chemical properties obtained from equations 9 to 13 below, including E_{HOMO}, E_{LUMO}, ΔE, χ, η, σ, and ΔN. You may calculate a molecule's electron-donor potential using its E_{LUMO} value. The donor molecule with a low-energy, unoccupied molecular orbital can readily donate electrons to an suitable acceptor molecule with a greater E_{HOMO}. [16]. In contrast to the experimental data, Table 1 shows that the E_{HOMO} value of thiourea (-0.215 eV) is larger than the E_{HOMO} value of thioureaH^+ (-0.430 eV).

Corresponding author. Tel: +2348065356180; e-mail: uzah2t@gmail.com
https://doi.org/ 10.22034/JCHEMLETT.2024.413932.1135

An element's E_{LUMO} value reflects how well a molecule can take in electrons. The easier it is for E_{LUMO} to receive electrons, the lower the value [17]. A corrosion inhibitor needs to have low values for ΔE but high values for in order to be effective. Additionally, when ΔN is lower than 3.6, the performance of inhibition as a function of electron transfer improves. In comparison to thiourea, ΔN 's thioureaH$^+$ has a larger value [18]. It also shows that the electron-exchange properties of thiourea and thioureaH$^+$ vary. In conclusion, the quanta chemical parameters provide strong support for the acquired experimental results discussed below.

Table 1. Density functional theory parameters of thiourea in the solvent phases and gas at B3LYP/6-311G+(d,p).

Phase	**E_{HOMO}**	**E_{LUMO}**	**ΔE (eV)**	**σ (eV^{-1})**	**χ (eV)**	**η (eV)**	**ΔN (eV)**	**μ (Debye)**
Gas	-0.215	-0.024	0.191	0.095	0.149	10.48	0.33	5.48
Solvent	-0.430	-0.246	0.183	0.092	0.338	10.92	0.30	7.26

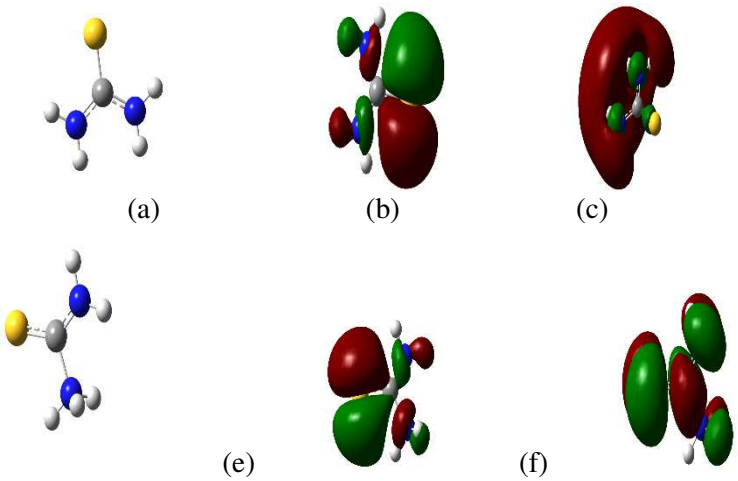

Fig. 1. Optimized, HOMO and LUMO structures of the thiourea (a, b, c) and protonated thiourea (d, e, f) respectively.

2.1 Monte Carlo Simulation

The pictures in Figure 2 show that thiourea adsorb tightly and lie parallel to the surface of iron.The ability of thiourea to transmit electrons to the metal surface is mostly due to its S and N atoms, as seen in Figure 2. Inhibitor molecules are quasi-substituted for water molecules during the adsorption of inhibitors on the metal surface in a solution. due to the fact that water (Table 2) has a lower adsorption energy (-1.044 kJ mol^{-1} against. -488.0 kJ mol^{-1}). This makes it possible to protect the metal surface [19,20].The energy needed to remove an adsorbate of a particular component is also indicated by the differential adsorption energy ((dE_{ad}/dN_i), which is also present. Since H_2O has a low absolute value of (dE_{ad}/dN_i), inhibitor molecules can gradually replace the water molecule. The most important adsorption characteristic is adsorption energy, which has two parts: the rigid adsorption energy needed to initially adsorb the inhibitor onto the steel surface, and a small deformation energy brought on by the inhibitor relaxing on the surface of iron (Fe (110)). An increase in the absolute value of the adsorption energy reflects strong adsorption behavior.

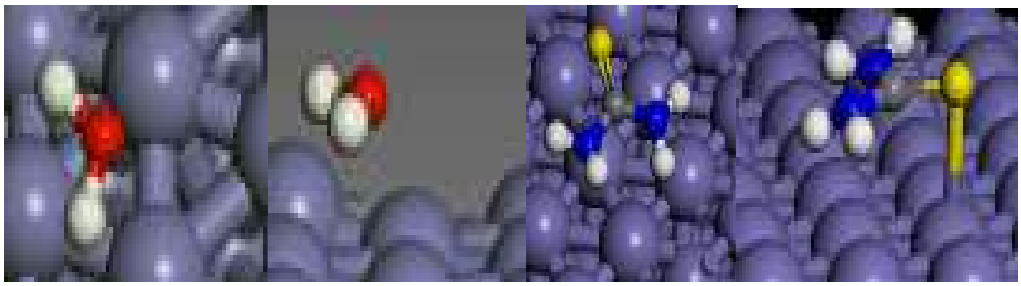

(a) Water (b) Thiourea

Fig. 2. Top and sideview of the adsorption of the (a) water and (b) thiourea molecule on Fe (110) surface using the Monte Carlo simulation

Table 2. Parameters calculated for adsorption via the M C simulation of water and thiourea on Fe (110) (kJ mol^{-1})

	Energy				
Compound	**Total**	**Adsorption**	**Rigid Adsorption**	**Deformation**	**dE_{ad}/dN_i**
Thiourea	-1.667	-488.0	-443.1	-44.94	-48.44
Water	-174.9	-1.044	-176.7	-867.2	-103.9

2.2 Effect of Concentration

Gravimetry and EIS were employed to examine how inhibitor concentration affected inhibitory activity. Figure 3 displays the results of the gravimetric test for metal in sulphuric acid solution carried out in both without and with of thiourea and thiourea + $ZnCl_2$ inhibitors at varied doses. Figure 4a, b demonstrates that the rate of corrosion decreased as the studied inhibitor's concentration rose, leading to an increase in efficacy. This implies that both inhibitors are likely working to impede corrosion. Mild steel was subjected to EIS tests in the acid medium at 298 K in both without and with various inhibitor dosages in order to validate the results of study on weight loss. The associated Nyquist graphs (Figure 3), which demonstrate that the R_{ct} mechanism and C_{dl} are the crucial factors governing corrosion, can be shown to contain a single capacitive loop. Furthermore, these impedance spectra have a consistent pattern across all concentrations investigated, showing that the mechanism of corrosion is mostly unaffected [19,20].. The width of the curves, however, dramatically rises when the two inhibitors are combined, indicating a higher inhibitive activity with a synergistic effect [21]. The obtained data are shown in **Error! Reference source not found.**. These are the formulas used to calculate the values of C_{dl}.

$$C_{dl} = \frac{1}{f_{max} \times 2\pi \times R_{ct}} \quad (1)$$

Where, C_{dl} is the double-layer capacitance, f_{max} is the frequency value at which the imaginary component of the impedance is greatest

$$\%\, I.E_{EIS} = \frac{[R]_{ct(inh)} - [R]_{ct(uninh)}}{[R]_{ct(inh)}} \times 100 \quad (2)$$

Where, $R_{ct(uninh)}$ (Ωcm^2) and $R_{ct(inh)}$ (Ωcm^2) are respectively resistances to charge transfer with and without an inhibitor. Table 3 makes it evident that the R_{ct}values rise according to the inhibitor concentration. Particularly clear is the upward trend in R_{ct}values for the mixture of thiourea and $ZnCl_2$ [22]. The inhibitors' potential adhesion to the medim/metal contact may be the cause of these results. The synergistic adsorption of two inhibitors on the surface of mild steel may result in the formation of a potent protective layer, even if the adsorption behaviour is more obvious when there are two inhibitors present. Additionally, the values of C_{dl} show a tendency to fall as inhibitor concentrations rise [23]. As a result, as inhibitor concentrations rise, so do inhibition efficiency, reaching 61.68 % for thiourea and 81.45 % for thiourea + 5 mM $ZnCl_2$ at 0.0006 M and 0.0006 M, respectively. These EIS study results are exactly in line with what the gravimetry data indicated.

Table 3. EIS data for steel insulphuric acid solution containing various concentrations of thiourea and thiourea + $ZnCl_2$ at 298 K

(a)

	Conc (M)	R_s (Ω cm^2)	R_{ct} (Ω cm^2)	C_{dl} (μF cm^2)	% IE
Thiourea	Blank	186.4	267.4	221.4	-
	2×10^{-4}	161.6	585.6	125.2	54.34
	4×10^{-4}	158.3	633.7	123.6	57.81
	6×10^{-4}	157.1	697.6	118.8	61.68
	8×10^{-4}	158.9	804.8	116.8	66.78
	1×10^{-3}	152.1	881.1	112.4	69.66
Thiourea + Zn^{2+}	2×10^{-4}	164.7	921.1	117.8	70.97
	4×10^{-4}	160.1	120.2	115.3	77.82
	6×10^{-4}	157.5	144.1	110.9	81.45

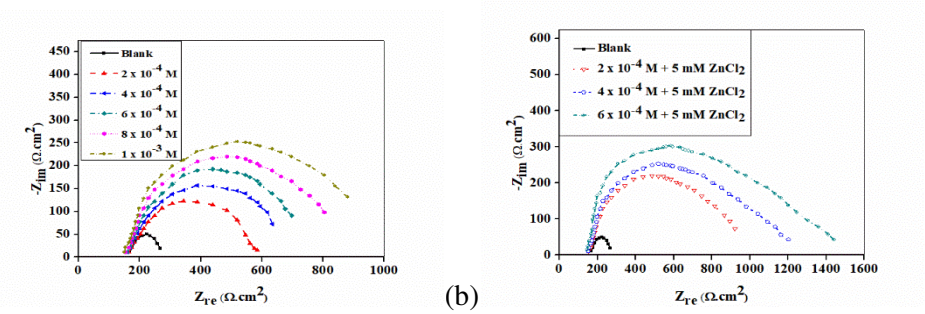

Fig. 3. EIS Nyquist plots of the corrosive mild steel in 0.5 M sulphuric acid solution and various concentrations of (a) thiourea alone (b) thiourea + $ZnCl_2$ at 298 K

Table 4. % IE of mild steel corrosion using thiourea and thiourea + $ZnCl_2$ at various temperatures.

Concentration	% IE Thiourea				Thiourea + Zn^{2+}			
(M)	298 K	308 K	318 K	328 K	298 K	308 K	318 K	328 K
2×10^{-4}	50.80	49.92	47.27	44.68	74.67	74.25	72.42	69.66
4×10^{-4}	54.93	53.49	51.53	49.11	79.87	77.68	76.08	73.53
6×10^{-4}	59.82	58.73	57.03	54.61	86.38	85.41	83.18	81.19
8×10^{-4}	64.82	62.97	60.88	59.19	91.10	88.93	87.19	84.49
1×10^{-3}	73.51	72.65	70.37	69.55	98.92	97.02	94.31	91.14
5.10^{-3} Zn^{2+}	48.72	45.37	42.64	38.33	-	-	-	-

2.3 Effect of Temperature

Fig. 4 shows how the inhibitory capacities of thiourea and thiourea + $ZnCl_2$ decrease with increasing temperature. The % IE of thiourea drops from 73.51 to 69.55 % and that of thiourea + $ZnCl_2$ decreases from 98.92 to 91.14 %, specifically, when the concentration is 0.001 M and the temperature varies between 298 and 328 K. This behavior can be explained by the fact that when temperature rises, the corrosion inhibitors disintegrate from the steel surface, leaving the metal unprotected and their ability to prevent corrosion to decline [24].

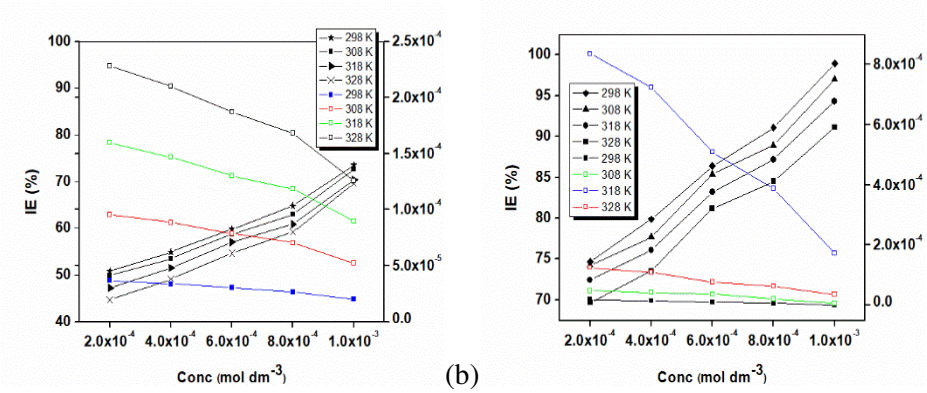

Fig. 4. Effect of concentration and corrosion rate on the inhibitive efficacy of (a) thiourea and (b) thiourea + $ZnCl_2$ on mild steel in the acid soluton$_4$

2.4 Kinetic andThermodynamics Considerations

The rate of mild steel corrosion in the acid media was utilised to compute the activation energy ((Ea) using the Arrhenius equation (3).

$$lnC_R = lnA - \frac{Ea}{RT} \quad (3)$$

$$In\left(\frac{C_R}{T}\right) = \left(\frac{R}{Nh}\right) exp\left(\frac{\Delta S_{ads}}{R}\right) exp\left(\frac{-\Delta H_{ads}}{RT}\right) \quad (4)$$

where, C_R is the rate of corrosion, A is The universal gas constant, R, is $R(8.314J\ mol^{-1}K^{-1})$, the Arrhenius constant is A, h is the plank's constant, and N is Avogadro's number. T is the absolute temperature. The activation energy values were determined from the slope of - Ea /R on the Arrhenius plot of ln C_R against 1/T (Figure 5). The energy of activation for an inhibited solution is higher than it is for an unrestricted solution if an inhibitor's ability to inhibit diminishes with rising temperature [25]. Table 5 contains the E_a results for 0.5 M H_2SO_4. The Ea values in the acid solutions are higher when thiourea is present than when it is not. The energy barrier for corrosion reaction is demonstrated by the inverse correlation between the rise and inhibitor concentration. Equation (7) is used to determine the adsorption free energy when computing the activation enthalpy and entropy for metal dissolution using the transition state equation (4). This leads to a straight line when plotting In (C_R/T) against 1/T. The values of ΔH_{ads} and ΔS_{ads}were derived from the slope and intercept of the plot, respectively. The computed activation enthalpy (ΔH_{ads}) is obviously involved in the physisorption process on the mild steel surface, as shown in Table 5. Electrostatic forces are reacting between the charged steel and the charged inhibitors. because as the temperature rises, they are easily separated from the metal surface The value of ΔH_{ads} is usually accepted to be more negative than -80 kJ mol^{-1} for chemisorption and less negative than -40 kJ mol-1 for physisorption [26]. Entropy (ΔS_{ads}) values for the inhibitors that are negative imply that there was a reduction in randomness during the transition from the reactants to the activated complex [27]. The corrosion of mild steel stopped by inhibitors also revealed a lot of water molecules on mild steel surface being displaced by inhibitor molecules, according to the large negative values of ΔS_{ads}.

Table 5. Values of thermodynamic and kinetic parameters of corrosive mild steel inhibition applying thiourea and thiourea + $ZnCl_2$

(a)

Conc.	Thiourea			Thiourea + Zn^{2+}		
	Ea /(kJmol^{-1})	ΔH_{ads} /(kJ mol^{-1})	-ΔS_{ads} /(J mol^{-1})	Ea /(kJmol^{-1})	ΔH_{ads} /(kJ mol^{-1})	-ΔS_{ads} /(J mol^{-1})
Blank	45.7	43.2	177.6	45.7	43.2	177.6
0.0002	49.1	46.3	173.2	50.6	47.5	175.7
0.0004	49.2	46.4	173.6	53.0	50.4	166.9
0.0006	49.1	46.4	174.6	52.5	49.9	171.1
0.0008	49.7	47.3	172.6	60.6	57.8	178.7
0.001	49.9	47.0	176.1	83.1	83.1	236.2

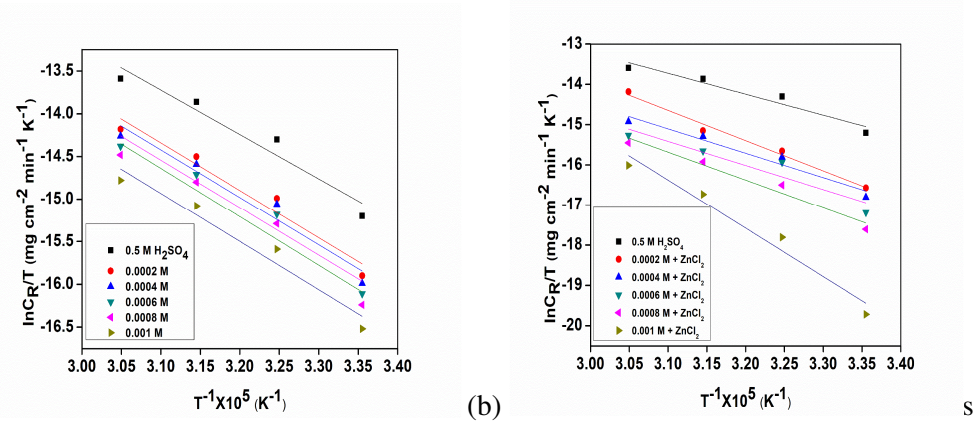

Fig. 5. Arrhenius plots ln C_R vs 1/T of (a) thiourea alone and (b) thiourea + $ZnCl_2$ for mild steel in sulphuric acid medium at various concentrations for 6 h

2.5 Adsorption Isotherm

The isotherms of thiourea adsorption on mild steel in a 0.5 M H_2SO_4 solution were investigated to identify the most likely mechanism for the interaction between organic corrosion inhibitors and the surface of metal. The most popular adsorption isotherms, Temkin, El-Awady, Freundlich, and Langmuir, were fitted to the data, and coefficients of determination (R^2) (Table 6) were obtained.to discover the best fits. [28]. Fig. 6a,b demonstrates that the Langmuir and Freundlich adsorption isotherms offered the best match for thiourea and thiourea + $ZnCl_2$ data respectively, According to [29], the Freundlich constants, which have to do with adsorption intensity, vary with the material's heterogeneity. It has been demonstrated that a desirable value for this constant should be near to 0.6 [18]. Tables 6 do not contain a value that comes close to it. The expressions for Langmuir and Freundlich isotherms in equations (5) and (6) are,

$$\frac{C}{S_c} = \frac{1}{K_{ads}} + C \qquad (5)$$

$$logS_c = \log K_{ads} + \frac{1}{n} logC \qquad (6)$$

where K_{ads} is the adsorptive equilibrium constant, Sc is the degree of surface covering, and C is the concentration of inhibitor and n is the number of displaceable water molecules by molecules of inhibitor on the metal surface. The free energy of adsorption (ΔG_{ads}) was computed based on Equation (7):

$$\Delta G_{ads} = -RTln(55.5K) \qquad (7)$$

Where, T = absolute temperature, R = universal gas constant, and the number 55.5 indicates the water's molar concentration. The values of ΔG_{ads} for thiourea and thiourea + $ZnCl_2$ ranged from -9.22 kJ mol^{-1} to -15.66 kJ mol^{-1} (Table 6), demonstrating the spontaneity of the adsorption processes. [30]. The numbers additionally illustrated the process's reversibility (physisorption) [31].

Table 6. Parameters of Langmuir and Freundlich adsorption isotherm for thiourea and thiourea + $ZnCl_2$ as inhibitor of mild steel corrosion in acid medium at different temperatures.

(a)

Isotherm	Temp.	R^2	Intercept	Slope	K_{ads}	Isotherm constant	ΔG_{ads}
Langmuir (Thiourea)	298	0.9991	0.0001	1.6863	10.000		-15.66
	308	0.9985	0.0002	2.0375	5.0000		-13.94
	318	0.9980	0.0003	2.2678	3.333.3		-13.39
	328	0.9963	0.0006	1.8274	1.666.6	n	-12.35
Freundlich (Thiourea + Zn^{2+})	298	0.9359	0.4755	0.1654	-0.7434	6.0459	-9.22
	308	0.9148	0.4531	0.1607	-0.7916	6.2228	-9.69
	318	0.9272	0.4401	0.1599	-0.8208	6.2539	-10.10
	328	0.9399	0.4401	0.1642	-0.8208	6.0901	-10.41

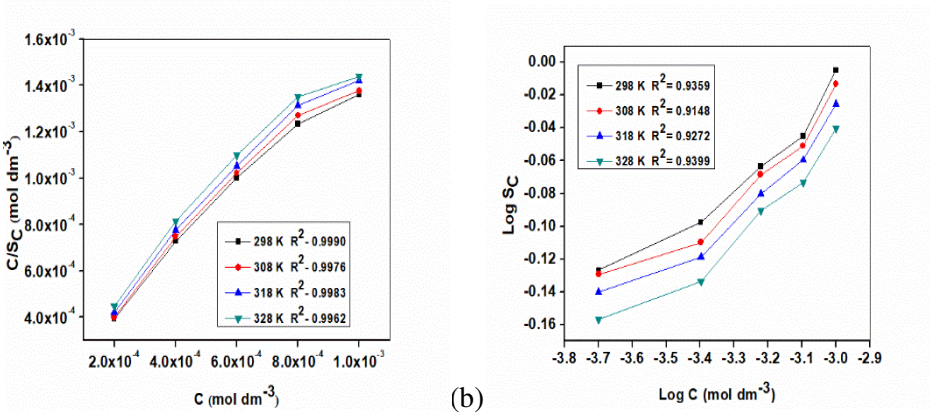

Fig. 6. Langmuir and Freundlich adsorption isotherms for adsorption of (a) thiourea alone (b) thiourea + $ZnCl_2$ on mild steel in 0.5 M H_2SO_4 solution at various temperatures

2.6 Synergism effect parameters.

The synergism parameters (S_P) were estimated using the following equation (8) based on the acquired surface coverage values.

$$S_P = \frac{1 - S_1 - S_2 + (S_1 \times S_2)}{1 - S_{1+2}} \qquad (8)$$

Where, S_1 and $S_2$are the surface coverage in each component's independent presence, while $S_{1+2}$is the degree of surface coverage in their coexistence. As the concentration of thiourea rises, the synergism parameter, S_P, rises as well until it reaches its maximum value.

Table 7. Synergism parameter (S_P) for various concentrations of thiourea + $ZnCl_2$ as mild steel corrosion inhibitor.

Thiourea (M)	**Zn^{2+} (mM)**	**S_P**			
		25°C	**35°C**	**45°C**	**55°C**
0.0002	5	1.00	1.06	1.10	1.12
0.0004	5	1.15	1.14	1.16	1.19
0.0006	5	1.51	1.55	1.47	1.49
0.0008	5	2.03	1.83	1.75	1.62
0.001	5	2.58	2.02	2.99	2.12

The majority of S_P values at increasing concentrations of thiourea are obviously more than 1, as shown in Table 7, demonstrating the synergistic nature of the corrosion inhibition caused by the complex of thiourea and $ZnCl_2$ [32]. It is obvious that as experimental temperature rises, the synergism parameter's value rises as well.

2.7 Scanning electron microscopy (SEM) Analysis

To compare the surface morphology before and after the inhibitor was applied at 298 K, mild steel was immersed in 0.5 M H_2SO_4 for 6 hours. Figure 7(b) illustrates the severely damaged mild steel surfaces caused by the generation of corrosion products following immersion in acid solution. The polished steel obtained by SEM without exposure to corrosive conditions is shown in Figure 7(a), which makes it clearer that the metal sample before immersion seems smooth and has some scratches of abrading on the metal surface. Nevertheless, the surface of steel in Figure 7(c) SEM picture following immersion in sulphuric acid solution with 0.001 M thiourea + 5 mM $ZnCl_2$ only suffered slight deterioration. There was less contact between the aggressive medium and the steel as a result of the mild steel's greater surface area. So mild steel corrosion can be successfully avoided with a sufficiently absorbent protective layer [33].

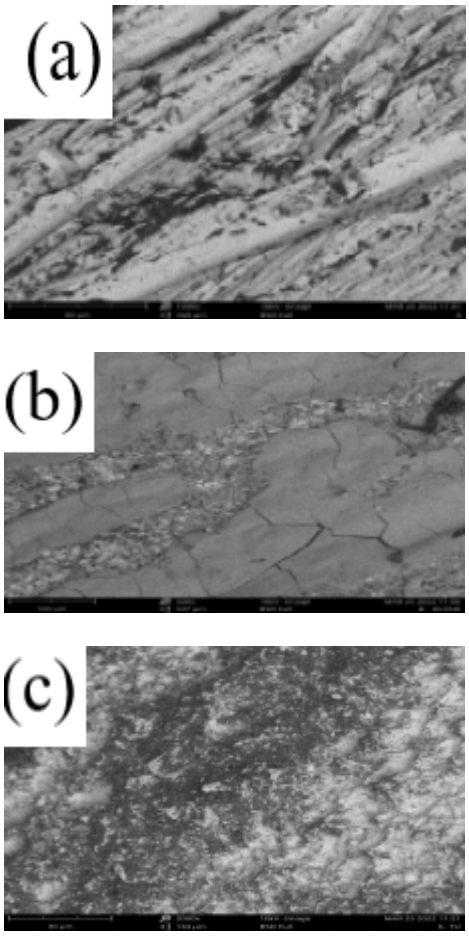

Fig. 7. SEM pictures of mild steel (a) before immersion (b) after immersion in acid soluton and (c) latter immersion in 0.001 M thiourea + $ZnCl_2$ solution for 6 h.

2.8 Fourier Transfer Infrared Spectroscopy (FTIR) Analysis

Figure 8 depicts the FTIR spectrum of the thiourea-containing coating that formed on the mild steel surface following immersion in sulphuric acis solution. The frequency of the C=S stretching has changed from 730.19 to $582.54cm^{-1}$The frequency of the N-H stretch has changed from 3076.41 to $3424.15\,cm^{-1}$). The frequency of the C-N stretching has changed from $633.41\ and\ 2110..01\ cm^{-1}$ to $2363.96cm^{-1}$This shows that the sulphur atom of the C=S group and the nitrogen atom of the N-H group on the mild steel surface have coupled with thiourea to produce the Fe^{2+} - Thiourea compound. complex. Accordingly, the FTIR analysis reveals that the protective coating is made up of a Fe^{2+}-thiourea complex that has developed on the metal surface. [34].

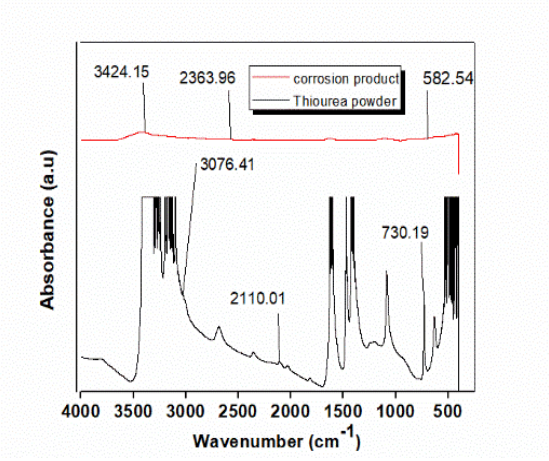

Fig. 8. FTIR spectrum of thiourea powder and corrosion product

3. Experimental

3.1. Chemicals

The corrosive medium, 0.5 M sulphuric acid, was made by combining laboratory-grade sulfuric acid with

distilled water. without additional purification, thiourea (99%) was utilised (Tianjin Kermel Chemical Reagent Company, China). Inhibitor doses ranging from 0.0002 to 0.001 M were added to a 0.5 M sulphuric acid solution to form the testing solution. On the other hand, the absence of inhibitors in the solution was referred to as "blank."

3.2 Quantum Chemical Computations

The Gaussian 09W software was used to make calculations for quantum chemistry. Using the generalized gradient approximation (GGA) functional of BLYP/6-311G+(d, p) of the density functional theory (DFT), we performed geometrical optimizations and frequency computations. The effect of the solvent was taken into account to obtain

more trustworthy data. Investigations were also made into the quantum chemical properties resulting from the optimized structures [18].

$$\Delta E = E_{LUMO} - E_{HOMO} \quad (9)$$

$$\sigma = \frac{2}{\Delta E} \quad (10)$$

$$\eta = \frac{\Delta E}{2} \quad (11)$$

$$\chi = \frac{-(E_{HOMO} + E_{LUMO})}{2} \quad (12)$$

$$\Delta N = \frac{(\chi_{Fe} - \chi_{inh})}{2 \times (\eta_{Fe} - \eta_{inh})} \quad (13)$$

Where, $\eta_{Fe} = 0\ eV$ and $\chi_{Fe} = 7$ in case of iron, ΔE = energy gap, E_{LUMO} = lowest unoccupied molecular orbital energy, E_{HOMO}= highest occupied molecular orbital energy, σ= global softness, η= absolute hardness, χ = absolute electronegativity, ΔN = number of electrons transferred

3.3 Monte Carlo Simulations.

Using Materials Studio software's adsorption locator module (version 2020, BIOVIA), the adsorption behavior of thiourea molecules on iron surface was investigated. The simulations were carried out in a simulation box with periodic boundary conditions, measuring 41.15 × 36.58 × 29.97 inches, to recreate an interface segment representative of the interface free from arbitrary boundary effects. The structures of every system component were improved using COMPASS, the first ab initio forcefield capable of precisely predicting chemical and condensed-phase characteristics for a range of chemical systems [35].

3.4 Weight loss Measurement

Manganese (0.56), phosphorus (0.04), carbon (0.27), silicon (0.25), sulphur (0.04), and iron make up the bulk of the mild steel coupons' (wt %) composition. Mild steel coupons measuring 4.1 cm x 2.1 cm x 0.08 cm were manually press-cut as part of the process and were grounded using Emery paper. The weighed coupons were immersed in the acidic medium with and without inhibitors for six hours at 298, 308, 318, and 328 K. Specimens were taken out of the acid solution after the experiment, washed with acetone, allowed to dry by air, and then weighed [36].The corrosion rate and inhibition efficiency are calculated using Equations (14) through (16) using the mean weight loss.

$$C_R = \frac{W_o - W_1}{At}\ (mg\ cm^{-2}\ min^{-1}) \quad (14)$$

where, C_R is the corrosion rate, A is the total exposed area in cm^2, W_o is the initial weight before immersion, W_1 is the final weight after immersion, t is the exposed time in minutes.

$$S_C = \left(1 - \frac{[W]_{inh}}{[W]_{uninh}}\right) \quad (15)$$

$$\%\ IE = S_c \times 100 \quad (16)$$

where $[W]_{uninh}$= mass loss in the absence of inhibitors, $[W]_{inh}$= mass loss in the presence of inhibitors, S_C= Surface coverage

3.5 Electrochemical impedance spectroscopy (EIS) measurement

Electrochemical measurements were performed using a Bio Logic VMP potentiostat electrochemical analyzer model SP- 300 with EC- Lab software in a conventional three-electrode cell. The active electrode was a mild steel coupon. Graphite electrode and Ag/AgCl (3 M KCl) were used as the reference and counter electrodes, respectively. The EIS measurements were carried out in a potentiostatic environment, from 100 kHz to 0.1 Hz. Zsimpwin 3.10 was used to match the impedance data [37,38].

3.6 SEM Analysis

By using scanning electron microscopy (SEM) analysis, the surface morphology of the layers formed on coupon was investigated in both the absence and presence of the 0.001 M inhibitor concentration. The specimens were removed, dried, and examined by the JSM-6360 LV apparatus using SEM photographs of their surfaces [33].

3.7 FTIR Analysis

The Furier Transfer Infrared Spectroscopy (FTIR) data was merged with a data table created using FTIR spectra that were made available to the public. The mild steel coupons were removed from the 100 mL of 0.001 M thiourea after 6 hours and dried. After being gently scraped off, the thin film that had amassed on the metal

surfaces was then properly mixed with KBr to make it consistent throughout [17].

4. Conclusion

The investigated inhibitor shown a strong ability to inhibit mild steel surfaces from corrosion when in touch with sulfuric acid solution. Along with the surface analysis characterisation, theoretical and experimental methods supported this conclusion. From this research, it may be inferred that:

i. Thiourea acts as an inhibitor for mild steel in a 0.5 M sulphuric acid medium.
ii. The efficiency of the inhibition rises with the concentration of the inhibitors.
iii. A synergistic effect increased the inhibitory efficacy when zinc ions were added to thiourea.
iv. Both the Langmuir and Freundlich adsorption isotherms were obeyed by the adsorption of thiourea alone and in conjunction with zinc ions.
v. Physisorption was involved in the inhibitory process, according to the thermodynamic characteristics estimated from the adsorption isotherms.

.

References

[1] C. Liu, R I. Revill, Z. Liu D. Zhang, X. Li and H. Terryn. Effect of inclusions modified by rare earth elements (Ce, La) on localized marine corrosion in Q460NH weathering steel. *Corr. Sci.* 129, (2017) 82–90.

[2] Y. Ye, Z. Liu, W. Liu, D. Zhang, H. Zhao, L. Wang and X. Li. Superhydrophobic oligoaniline-containing electroactive silica coating as pre-process coating for corrosion protection of carbon *steel. Chem.l Eng. J.* 348 (2018) 940–951.

[3] L. Chen, D. Lu and Y. Zhang "Organic Compounds as Corrosion Inhibitors for Carbon Steel in HCl Solution. A Comprehensive Review. *Materials.* 15 (2022) 2023.

[4] N. Chaubey, S. A. Qurashi, D. S. Chauhan and M. Quraishi. Frontiers and advances in green and sustainable inhibitors for corrosion applications: A critical review. *J. Mol.r Liq.* 321 (2021) 114385.

[5] S. H. Alrefaee, K.. Y. Rhee, C. Verma, M. Quraishi and E. E. Ebenso. Challenges and advantages of using plant extract as inhibitors in modern corrosion inhibition systems: Recent advancements. *J. Mol.r Liq.,* 321 (2021) 114666.

[6] M. M. Solomon and S. A. Umoren. Enhanced corrosion inhibition effect of polypropylene glycol in the presence of iodide ions at mild steel/sulphuric acid interface. *J. Environ. Chem.l Eng.,* 3 (2015) 1812–1826.

[7] Z. Salarvand, M. Amirnasr, M. Talebian, K. Raeissi and S. Meghdadi. Enhanced corrosion resistance of mild steel in 1M HCl solution by trace number of 2-phenylbenzothiazole derivatives: experimental, quantum chemical calculations and molecular dynamics (MD) simulation studie.s *Corr. Sci.,* 114, (2017) 133-145.

[8] A. S. Raja, S. Rajendran, R. Nagalakshmi, J. A. Thangakani and M. Pandiarajan. Eco-friendly inhibitor glycine- Zn2+ system controlling corrosion of carbon steel in well water. *Eur. Chem.l Bull.,* 2 (2013) 130 - 136.

[9] R. S. Susai, R. Mary, A. Noreen and R. Ramaraj. Synergistic corrosion inhibition by the sodium dodecylsulphate–Zn^{2+} system. *Corr. Sci.,* 44, no. 10(2002) 2243-2252.

[10] S. Manov, A. M. Lamazouere and L. Aries. Electrochemical study of the corrosion behaviour of zinc treated with a new organic chelating inhibitor. *Corr. Sci.,* 42, (2000) 1235–1248.

[11] A. Kadhim, A. Al-Amiery, R. Alazawi, M. Al-Ghezi and R. Abass, Corrosion inhibitors. A review. *Int. J. Corr. Scal. Inhib,* 10 (2021) 54–67.

[12] M. Hanoon, A. M. Resen, A. A. Al-Amiery, A. A. H. Kadhum and M. S. Takriff. Theoretical and Experimental Studies on the Corrosion Inhibition Potentials of 2-((6-Methyl-2-Ketoquinolin-3-yl)Methylene) Hydrazinecarbothioamide for Mild Steel in 1 M HCl.. *Prog. Color*, *Colorants,* 15 (2022) 21-33.

[13] F. G. Hashim, T. A. Salman, S. B. Al-Baghdadi, T. Gaaz and A. A. Al-Amiery. Inhibition effect of hydrazine-derived coumarin on a mild steel surface in hydrochloric acid. *Tribologia,* 37 (2020) 45–53.

[14] A. M. Resen, M. Hanoon, R. D. Salim, A. A. Al-Amiery, L. M. Shaker and A. A. H. Kadhum. Gravimetrical, theoretical, and surface morphological investigations of corrosion inhibition effect of 4-(benzoimidazole-2-yl) pyridine on mild steel in hydrochloric acid. Koroz Ochr. Mater., 64 (2020) 122-130.

[15] X. Yue, Q. Wei, Y. Lu, M. Duan, H. Wang and J, Xie. The Synergistic Inhibition Effect between Imidazoline and 2-Mercaptoethanol on Carbon Steel Corrosion in CO_2-saturated 3.5% NaCl solution. *Int. J. Electrochem. Sci.*, 17 (2022) 1—8

[16] A. S. Fouda, M. A. Ismail, A. M. Temraz and A. S. Abousalem. Comprehensive investigations on the action of cationic terthiophene and bithiophene as corrosion inhibitors: Experimental and theoretical studies, *New J. Chem.*, 43 (2019) 768–789.

[17] R. Epshiba, R. A. Peter Pascal and S. Rajendran. Electrochemical and surface analysis studies on corrosion inhibition of carbon steel in well water by curcumin. *Int. J.* Adv. *Appl. Sci.,* 5, (2017) 1-11.

[18] T. T. Uzah, J. I. Mbonu, T. E. Gber and H. Louis. Synergistic effect of KI and urea on the corrosion protection of mild steel in 0.5 M H_2SO_4: Experimental and computational insights. *Resul. Chem.*, 5(2023) 1-9.

[19] S. K. Saha and P. Banerjee. Introduction of newly synthesized Schiff base molecules as efficient corrosion inhibitors for mild steel in 1 M HCl medium: An experimental, density functional theory and molecular dynamics simulation study. *Mater.s Chem. Front.,* 2 (2018) 1674–1691.

[20] A. Fouda, A. Tilp and A. Al-Bonayan. Conocarpus Erectus Extract as an Eco-Friendly Corrosion Inhibitor for Aluminum in Hydrochloric Acid Solution. *Biointerface* Res. *Appl. Chem.*, 11 (2021) 10325 – 10340.

[21] R. Hussein, M. Abou-Krisha and T. Yousef "Theoretical and Experimental Studies of Different Amine Compounds as Corrosion Inhibitors for Aluminum in Hydrochloric Acid. *Biointerface* Res. *Appl. Chem.*, 11, (2021) 9772 – 9785.

[22] M. Wasim S. Shoaib, N. M. Mubarak, A. Inamuddin and A. M. Asiri. Factors influencing corrosion of metal pipes in soils. *Environ. Chem. Lett.*, 16 (2018) 861-879.

[23] B.V. Appa Rao and R. M. Narsihma. Formation, characterization and corrosion protection efficiency of self-assembled 1-octadecyl-1H-imidazole films on copper for corrosion protection. *Arab. J. Chem.*, 10 (2017) S3270-S3283.

[24] A. A. Alamier, Investigations on corrosion inhibitory effect of newly quinoline derivative on mild steel in HCl solution complemented with antibacterial studies. *Biointerface* Res. *Appl. Chem.*, 12 (2022) 1561 – 1568.

[25] A. S. Fouda, M. Abdel Azeem S. A. Mohamed, A. El-Hossiany and E. El-Desouky. Corrosion Inhibition and Adsorption Behavior of Nerium Oleander Extract on Carbon Steel in Hydrochloric Acid Solution. *Int. J. Electrochem. Sci.*, 14 (2019) 3932 – 3948

[26] Q. H. Dinh, T. Duong and N. P. A. Cam. Study of 1-Benzyl-3-phenyl-2-thiourea as an Effective Steel Corrosion Inhibitor in 1.0M HCl Solution. *J. Chem.* (2021) 1-14.

[27] K. Shalabi, A. M. Helmy, A. H. El-Askalany and M. M. Shahba. New pyridinium bromide mono-cationic surfactant as corrosion inhibitor for carbon steel during chemical cleaning: Experimental and theoretical studies. *J. Mol. Liq.*, 293 (2019) 1-10.

[28] M. H. Sliem, N. M. El Basiony, E. G. Zaki, M. A. Sharaf and A. M. Abdullah. Corrosion inhibition of mild steel in sulfuric acid by a newly synthesized schiff base: an electrochemical, DFT, and Monte Carlo simulation study. *Electroanalysis*. 32 (2020) 3145–3158.

[29] M. A. EL-Zekred, A. E. S. Fouda, A. M. Nofal and K. Shalabi. Plantago Major Extract as an Environmentally Friendly Inhibitor for the Corrosion of L-80 Carbon Steel in 0.5 M H_2SO_4 Media. *Biointerface* Res. *Appl. Chem.*, 11(2021) 12186 – 12201.

[30] N. El Basiony, E. E. Badr, S. A. Baker and A. El-Tabei. Experimental and theoretical (DFT&MC) studies for the adsorption of the synthesized Gemini cationic surfactant based on hydrazide moiety as X-65 steel acid corrosion inhibitor. *Appl. Surf. Sci*, 539 (2021) 14824.

[31] J. Aslam, R. Aslam, I. H. Lone, N. R. Radwan, M. Mobin, A. Aslam and A. A. Alzulaibani. Inhibitory effect of 2-Nitroacridone on corrosion of low carbon steel in 1 M HCl solution: An experimental and theoretical approach. *J. Mater. Res. Techn.* 9 (2020) 4061-4075.,

[32] Y. Qiang, Y. Qiang, L. Guo, S. Zhang, W. Li, S. Yu and J. Tan. Synergistic effect of tartaric acid with 2,6-diaminopyridine on the corrosion inhibition of mild steel in 0.5 M HCl. *Sci. Rep.* 6 (2016) 33305.

[33] T. Duarte, Y. A. Meyer and W. R. Osório. The holes of Zn Phosphate and hot dip galvanizing on electrochemical behaviors of multi-coatings on steel substrates. *Metals*, 12 (2022) 863.

[34] S. Raju, R. Muralidharan and H. Krishnan. A comparative study on the spectral properties of thiourea potassium chloride and thiourea tartarate single crystals. *Int. J. ChemTech Res.*, 6, 9 (2014) 4212-4215.

[35] A. S. Fouda, M. A. Ismail, M. A. Khaled and A. A. El□Hossiany. Experimental and computational chemical studies on the corrosion inhibition of new pyrimidinone derivatives for copper in nitric acid, *Sci. Rep.*, 12 (2022) 16089.

[36] S. O. Adejo, S. G. Yiase, L. Leke, M. Onuche, M. V. Atondo and T. T. Uzah. Corrosion studies of mild steel in sulphuric acid medium by acidimetric method. *Int. J. Corr. Scal. Inhib.*, 8 (2019) 50–61.

[37] M. E. Mashuga, L. O. Olasunkanmi and E. E. Ebenso Experimental and theoretical investigation of the inhibitory effect of new pyridazine derivatives for the corrosion of mild steel in 1 M HCl. *J.Mol. Stru.*, 1136 (2017) 127−139. B. S. Mahdi, M. K. Abbass, M. K. Mohsin, W. K. Al-azzawi, M. M. Hanoon, M. Hliyil, H. Al-kaabi, L. M. Shaker, A. A. Al-amiery, W. R. Wan Isahak, A. H. Kadhum and M. S. Takriff Corrosion inhibition of mild steel in hydrochloric acid environment using terephthaldehyde based on schiff base: gravimetric, thermodynamic, and computational studies. *Molecules*, 27 (2022) 4857.